FEM SIMULATION OF FAILURE PROCESS of WOVEN CF/Epoxy LAMINATES

Risa Tanaka*,Naoyuki Watanabe **
***Graduate School of Aerospace Engineering, Tokyo Metropolitan University**
****Department of Aerospace Engineering, Tokyo Metropolitan University**

Keywords: *Woven CF/Epoxy laminates, thermal residual stress, homogenization method, transverse cracks, delamination, node separation method*

Abstract

3-D FEM simulation of the progressive failure process of woven CF/Epoxy laminates was carried out with including the thermal effects calculated by the homogenization method to investigate how important they are and which failure criterion is the best. Node separation method is adopted to simulate transverse cracks in fiber tows and delaminations between them. It is proved that the thermal residual stresses cannot be neglected in the failure process of woven CF/Epoxy laminates and that Hashin's criterion is more suitable and than Tsai-Wu's for this study from the comparison of the predicted location of transverse cracks. Through the simulation, the detailed behaviours of the failures were clarified including transverse cracks and successive delaminations between them. It was indicated that failures have not affected the fairly, but those of out-plain intensively under the progress failures.

1. Introduction

Woven CF/Epoxy laminates are generally more convenient than usual 2-D laminates because of their natural advantages of high interlaminar fracture toughness, notch insensitivity, excellent damage tolerance and great potential in spite of their low manufacturing cost. However, the failure mechanics of 2-D woven composites has not been fully evaluated because they have complicated geometric configurations in which the fiber direction changes gradually everywhere.

For the plain weave fabric composite, a variety of analytical models have been proposed. Chou and Ishikawa have proposed the mosaic model, the fiber undulation model and the bridging model, which are basically resulted from the classical lamination theory, and they calculated the macroscopic stiffness [1] [2]. Naik et al. suggested the element array model that can present a precise geometry and investigated thermo mechanical properties and fracture strength [3]-[5]. Although the values of in-plain elastic properties and stress distributions were evaluated from these analyses, these it was still difficult to investigate the accurate detail of plain-weave composites. Whitcomb and Chapman have analyzed the stress distribution by using 3-D FEM and complicated symmetrical boundary condition [6]. But their study didn't include the thermal effects. Watanabe et al. established FEM simulation of CF/Epoxy 3-D orthogonal interlocked fabric composites including the thermal effects by using the homogenization method. Although stiffness reduction method was adopted to simulate failures, the results were in good agreement with the experimental ones [7]. Tanaka improved their model for plain weave composites and showed node separation method is more effective in simulating the failures including delaminations than stiffness reduction method [8]. However, there hasn't been an evaluation of how important the thermal residual stresses are, of which failure criterion is the best for woven CF/Epoxy laminates.

In this research, the analysis of the progressive failure process is conducted by adopting 3-D FEM model including thermal residual stresses and by utilizing the homogenization method. Transverse cracks in fiber tows and delaminations between them are simulated with node separation method. Our objectives are to investigate aforementioned unsolved problems, the detailed behaviours of the failures and the changes in the elastic properties.

2. Theory

2. 1 Homogenization method

The homogenization method is a rigorous analytical method to the system composed of a large

amount of periodic microstructures, which is microscopically heterogeneous but can be regarded as macroscopically homogeneous. In the thermal-elasticity problem such as composites materials, this method gives considerably accurate equivalent elastic constants and accurate distributions for highly and locally changing stresses in the small base cell that is a minimum unit. The deformation and the distribution of the thermal residual stresses after the curing process cannot be obtained accurately by the usual FEM because it is very difficult to define the exact boundary condition to woven composites without using the homogenization method [9].

The stress-strain expression including the thermal effects and the strain-displacement relation obtained by the assumption of infinitesimal deformation is given as following

$$\sigma_{ij}^{\varepsilon} = E_{ijkl}^{\varepsilon}\left[\frac{1}{2}\left(\frac{\partial u_i^{e}}{\partial x_j}+\frac{\partial u_j^{\varepsilon}}{\partial x_i}\right)-\alpha_{kl}^{\varepsilon}\right] \tag{2.1}$$

where E_{ijkl}^{ε} and $\alpha_{kl}^{\varepsilon}$ are a elasticity tensor and thermal expansion coefficient of the body, respectively. Besides, superscript ε means a function of the total region including the micro structures in the remainder of this paper.

The solution the above thermo-elasticity problem is obtained by the weak form based on the principle of virtual work:

$$\int_{\Omega^{\varepsilon}} E_{ijkl}^{\varepsilon}\left(\frac{\partial u_k^{\varepsilon}}{\partial x_l}-\alpha_{kl}^{\varepsilon}\right)\frac{\partial v_i}{\partial x_j}d\Omega=\int_{\Omega^{\varepsilon}} f_i^{\varepsilon}v_i d\Omega+\int_{\Gamma_t} t_i v_i d\Gamma \tag{2.2}$$

where $u_k^{\varepsilon}(x)$ and $v_i(x,y)$ are a displacement and virtual displacement component respectively. f_i and t_i are a body forces and surface tractions. Eqs. (2.2) is assumed to satisfy the predicted geometrical boundary condition. The rigorous displacement field and stress field are assumed obey asymptotic expansion with respect to the parameter ε that is a measurement of the microscopic/macroscopic dimension ratio.

The solutions of thermo-elasticity problem are obtained as follows [9].

$$u^{\varepsilon}(x)=u^{0}(x,y)+\varepsilon u^{1}(x,y) \tag{2.3}$$

$$u_i^{0}(x,y)=u_i^{0}(x) \tag{2.4}$$

$$u_i^{1}(y)=-\chi_i^{kl}(y)\frac{\partial u_k^{0}(x)}{\partial x_l}-\Psi_i(y)\Delta T \tag{2.5}$$

$$\sigma^{\varepsilon}(x)=\sigma^{0}(x,y) \tag{2.6}$$

$$\sigma_{ij}^{0}(x,y)=\left(E_{ijkl}(x,y)-E_{ijpm}(x,y)\frac{\partial \chi_p^{kl}(x,y)}{\partial y_m}\right)\frac{\partial u_k^{0}(x)}{\partial x_l} - E_{ijkl}(x,y)\frac{\partial \Psi_k(x,y)}{\partial y_l}-E_{ijkl}(x,y)\alpha_k\Delta T \tag{2.7}$$

where ΔT is the temperature difference between the current state and the reference one. χ_i^{kl} is a characteristic displacement tensor, and Ψ_i is another characteristic displacement resulting from the thermal deformation. They are obtained by the following equations.

$$\int_{¥}\left(E_{ijkl}(x,y)-E_{ijpm}(x,y)\frac{\partial \chi_p^{kl}(x,y)}{\partial y_m}\right)\frac{\partial v_i(y)}{\partial y_j}dY=0 \tag{2.8}$$

$$\frac{1}{|Y|}\int_{¥}\chi_i^{kl}dY=0 \tag{2.9}$$

$$-\int_{¥}E_{ijkl}\frac{\partial \Psi_k}{\partial y_l}\frac{\partial v_i}{\partial y_i}dY=\int_{¥}E_{ijkl}\alpha_{kl}^{\varepsilon}\Delta T\frac{\partial v_i}{\partial y_i}dY \tag{2.10}$$

$$\frac{1}{|Y|}\int_{¥}\Psi_i dY=0 \tag{2.11}$$

where $|Y|$ is the volume of the base cell. In the three-dimensional formulation, the six sets of problem relating to $\chi_i^{kl}(k,l=1,2,3)$ must be obtained considering its symmetry. Consequently, Macroscopic homogenized elastic constants E_{ijkl}^{0} is defined as

$$E_{ijkl}^{0}=\frac{1}{|Y|}\int_{¥}\left(E_{ijkl}-E_{ijpm}\frac{\partial \chi_p^{kl}}{\partial y_m}\right)dY \tag{2.12}$$

and u_i^{0} is the macroscopic deformation when the body is assumed to be macroscopically homogeneous with above elastic constants E_{ijkl}^{0} as

$$\int_{\Omega}E_{ijkl}^{0}\left(\frac{\partial u_k^{0}}{\partial x_l}-\alpha_{kl}^{\varepsilon}\Delta T\right)\frac{\partial v_i(x)}{\partial x_j}d\Omega=\int_{\Omega}\tau_{ij}(x)\frac{\partial v_i(x)}{\partial x_j}d\Omega + \int_{\Omega}\sigma_{ij}^{t}(x)\frac{\partial v_i(x)}{\partial x_j}d\Omega+\int_{\Omega}b_i(x)v_i(x)d\Omega+\int_{\Gamma_t}t_i(x)v_i(x)d\Gamma \tag{2.13}$$

where

$$\tau_{ij}(x)=\frac{1}{|Y|}\int_{¥}E_{ijkl}\frac{\partial \Psi_k}{\partial y_l}dY \tag{2.14}$$

$$\sigma_{ij}^{t}(x)=\frac{1}{|Y|}\int_{¥}E_{ijkl}\alpha_{kl}\Delta T dY \tag{2.15}$$

and

$$b_i(x) = \frac{1}{|Y|}\int_{¥} f_i dY \tag{2.16}$$

where eqs. (2.14) and (2.15) are the terms expressing the microscopic and macroscopic thermal deformation effect. Consequently, the homogenized thermal expansion coefficient is given as

$$\alpha_{ij}^0 = \left[E_{ijkl}^0\right]^{-1} A_{ij}^0 \tag{2.17}$$

where A_{ij}^0 is called the homogenized thermal elastic coefficient and obtained by

$$A_{ij}^0 = \frac{1}{|Y|}\int_{¥}\left(E_{ijkl}(x,y)\alpha_{kl} + E_{ijkl}(x,y)\frac{\partial \Psi_k}{\partial y_l}\right)dY \tag{2.18}$$

As shown above, the macroscopic and microscopic problems are not coupled, i.e. the characteristic displacement χ^{kl} and Ψ can be computed within the base cell by solving eqs. (2.8) – (2.11), and the homogenized elastic constants are calculated by using eq. (2.12), which does not depend on the macroscopic deformation u_i^0. In this analysis, the body has a uniform cell structure in the whole domain so that the microscopic problems only need to be solved once.

2. 2 Composites material's criterion

Two criteria of composites materials are evaluated. The first one is Tsai-Wu's criterion [10] as follows:

$$f(\sigma) = F_{ij}\sigma_i\sigma_j + F_i\sigma_i = 1 \tag{2.19}$$

which can dustinguish tensile and compressive strength. Another is Hashin's criterion [11] that distinguishes four failure modes, tension fiber mode, compressive fiber mode, tensile matrix mode, and compressive matrix mode. A failure mode is categorized as that of fiber or matrix before distinguishing tensile or compressive mode. When the failure is applied to the matrix mode, it is remarkable to depend on the sum total of σ_{22} and σ_{33}. Therefore, it can be written

fiber mode:

$\sigma_{11} > 0$ then,

$$\left(\frac{\sigma_{11}}{F_{Lt}}\right)^2 + \frac{1}{S_{Lt}^2}\left(\sigma_{12}^2 + \sigma_{13}^2\right) = 1, or, \sigma_{11} = F_{Lt} \tag{2.20}$$

$\sigma_{11} < 0$ then,

$$\sigma_{11} = -F_{11} \tag{2.21}$$

matrix model:

$\sigma_{22} + \sigma_{33} > 0$ then,

$$\frac{1}{F_{Lc}^2}\left(\sigma_{22}+\sigma_{33}\right)^2 + \frac{1}{S_{Lc}^2}\left(\sigma_{23}^2 - \sigma_{22}\sigma_{33}\right)^2 + \frac{1}{S_{Lt}^2}\left(\sigma_{12}^2 + \sigma_{13}^2\right) = 1 \tag{2.22}$$

$\sigma_{22} + \sigma_{33} < 0$ then,

$$\frac{1}{F_{Lc}}\left[\left(\frac{F_{22}}{2S_{Lc}}\right)^2 - 1\right]\left(\sigma_{22}+\sigma_{33}\right) + \frac{1}{4S_{Lc}^2}\left(\sigma_{22}+\sigma_{33}\right)^2 + \frac{1}{S_{Lc}^2}\left(\sigma_{23}^2 - \sigma_{22}\sigma_{33}\right)^2 + \frac{1}{S_{Lt}^2}\left(\sigma_{12}^2 + \sigma_{13}^2\right) = 1 \tag{2.23}$$

3. Analytical Procedure

3. 1 Model for Base cell

Since woven composite materials have an out-of-plane undulation, it is very important to include their effects in predicting their behaviors, especially for initial failure strength, ultimate tensile strength and damage growth. In our analyses, the following model as mentioned below is considered in our analyses. The model is based on the periodic structure where adjacent layers are stacked in the same phase and shown in Fig. 1 together with each dimension. Consequently, the out-plain undulation is calculated based on the equations proposed by Naik [3]. The size of the base cell is $2.28\times2.28\times0.162$ mm. $T300$ and $Epoxy828$ as the material properties are tabulated in table 1. The fiber volume fraction within fiber tow is assumed to be 78%, and the material properties of tow are calculated by assuming that the fibers are placed in hexagonal array and by using the homogenization method. The properties are listed in table 2. The longitudinal tensile strength (F_{Lt}) is determined by considering the fiber volume fraction of a tow and the strength of CFRP unidirectional lamina. In this study, the estimated strength properties of tow are given in Table 3.

To judge if the elements are failed or not, both of the aforementioned criteria are utilized. Node separation method as mentioned in section 3.3 is adopted to simulate transverse cracks in fiber tows and delaminations between them. To consider tow' undulation of the tow both two kinds of coordinates are considered as shown in Fig.2. Axes of 1, 2 and 3 are the material coordinates, and axes of x, y and z are based on the global ones in this paper.

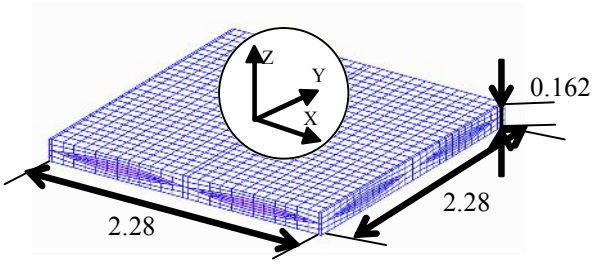

Fig. 1: Base cell

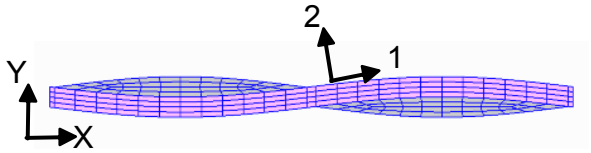

Fig. 2: Base cell and each coordinate

3. 2 Process of simulation

In the analysis, extended homogenization method with considering the thermal effect has been applied to woven laminates. The process of this simulation is as follows:

1) Homogenized elastic constants and distribution of thermal residual stresses are calculated by assuming that a temperature drop during the curring process is 100 K.
2) The model is subjected to uni-axial tensile load, where the loading direction is parallel to the x-axis.
3) After averaging obtained stress components in each finite element, the elements
are judged if they are failed or not with Tsai-Wu's or Hashin's criterion.
4) Some set of nodes are changed into double ones by Node separation method, to simulate microscopic failures including transverse cracks in the tows and delaminations between them.

Repeating this process from 1) to 4), until X fiber is expected to rupture somewhere.

In this procedure, the thermal residual stresses due to the temperature drop during the curring process are also calculated every repeating time so that they are changing with the new occurring transverse cracks and delaminations. The analysis is carried out by repeating this process until the ultimate failure of the unit cell occurs. If the fiber breakage occurs in the stuffers, the composite is assumed to suffer the ultimate failure. As for the prediction of fiber breakage, maximum stress criterion is applied to each element instead of the Tsai-Wu's or Hashin's criterion because it is assumed that the stress parallel to x-direction mostly contributes to this failure.

The number of elements and nodes of the base cell are 7424 and 33323. 20 nodes isoparametric elements are adopted and the numbers of integral points are 27 to calculate its own elastic constants. The base cell is made with Patran(MSB Co.Ltd) and it can be simulated with HP xw8000 workstation through our original program to include the homogenization method. Patran is also adopted to show deformations or stress distributions of the model after the simulation.

3. 3 Node Separation Method

Node separation method, "NSM", is adopted to simulate transverse cracks in fiber tows and delaminations between them. In this method, the common nodes on the face between the focused element and the adjacent one are changed into double nodes when both of these elements are judged to be failed. In Fig.2 (a) there are two elements, of which the left grey one is already judged to be failed and the adjacent transparent one hasn't. The common nodes on the interface between them are not changed into double ones here. Afterwards, like shown in Fig.2 (b), when both elements are judged to be failed, the common nodes are changed into double ones.

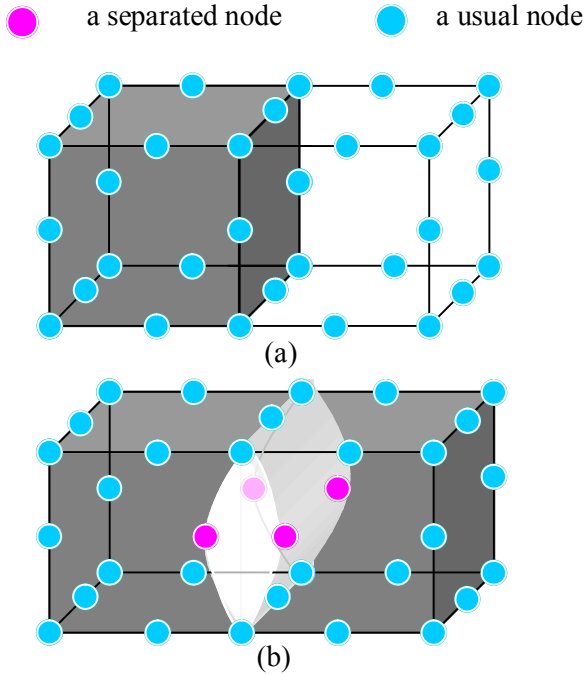

Fig. 3: Mechanism of NSM

Therefore the common nodes are changed when all elements relating the nodes are judged to be failed, so that it is assumed that transverse cracks are

simulated when all elements that lie around the predicted locations of the cracks are judged to be failed.

Thus, NSM is the method to extend transverse cracks as increasing failed elements during the simulation. Although it is well known that the crack propagation depends on the strain energy release rate, in this study it's not included but the stress criteria are utilized here. The delaminations between fiber tows are also an important phenomenon as a failure mode in woven composites and NSM is also adopted to simulate it in the same manner like the transverse crack.

Table 1: Material properties of carbon fiber and epoxy828

	E_L (GPa)	E_a (GPa)	G_{LT} (GPa)	G_{TT} (GPa)	ν_{LT}	$\alpha_L \times 10^{-5}$ $(1/T)$	$\alpha_L \times 10^{-5}$ $(1/T)$
T300	230	40	24	14.3	0.26	-0.07	3.00
Epoxy	3.5	3.5	1.3	1.3	1.3	6.45	6.45

Table 2: Material properties of Fiber tow (volume of fiber: $V_f = 0.78$)

E_L (GPa)	E_a (GPa)	G_{LT} (GPa)	G_{TT} (GPa)	ν_{LT}	ν_{TT}	$\alpha_L \times 10^{-7}(1/T)$	$\alpha_T \times 10^{-7}(1/T)$
180	17.8	7.66	6.34	0.276	0.431	-3.98	4.01

Table 3: Strength of Fiber tow (volume of fiber: $V_f = 0.78$)

	F_{Lt} (GPa)	F_{Lc} (GPa)	F_{Tt} (GPa)	F_{Tc} (GPa)	S_{LT} (GPa)	S_{TT} (GPa)
T300 Carbon Fiber	1.99	1.49	0.09	0.28	0.093	0.093

4. Importance of the thermal residual stresses

The simulation is performed under x-axis tensile force for two analyses with and without including the thermal residual stresses with Tsai-Wu's criterion to prove an importance of the thermal effect. In the analysis including the thermal effect, an accurate distribution of the stresses in the base cell is obtained through calculating with the homogenization method by considering periodic boundary conditions. The maximum tensile stress transverse to the fiber direction σ_2 and maximum shearing stress τ_{31} are 63.2MPa amounting to 70.2% of F_{Tt} and 50.5MPa to 56% of S_{Lt} respectively. The distribution of them based on a material coordinate are shown in Fig. 4 and Fig. 5. In Fig. 4 the maximum stress is observed on the edge of cross section of the fiber tows, because the narrow shape causes the stress concentration. The stresses are small on the other region as the tows become thicker in the out-plain direction. As observed in Fig. 5, the stress τ_{31} is generally high over the cross section inside the yellow ellipse, and the maximum occurs near the center.

With the applied stress of 36.6MPa an element in the Y fiber tows is first judged to be failed in both of the X and Y fiber tows. Then, transverse cracks occur first with the applied 71.2MPa in the Y fiber tows along the both thick lines in Fig. 6, which schematically shows a cross section of the Y fiber tow. Although it is well known the cracks occur as a straight line, but they are simulated in this analysis as

a curved line because of simplicity in the model is mesh division. In the other analysis without the thermal effect, these external stresses are 74.7MPa and 87.7MPa, respectively. But it is in the X fiber tows that an element is first judged to be failed and that the transverse cracks occur first. The result without the thermal effect is completely different and wrong. The transverse cracks should occur first in the Y fiber tow considering the actual thermal residual stresses since the thermal expansion coefficient along the fiber direction is a negative value and the applied stress is the x-axis tension. Furthermore, this fact was verified by some experiments and the analysis with the thermal effect can properly simulate the real behaviour.

Thus, it is proved that the thermal residual stresses calculated by using the homogenization method cannot be neglected in the failure process of woven CF/Epoxy laminates.

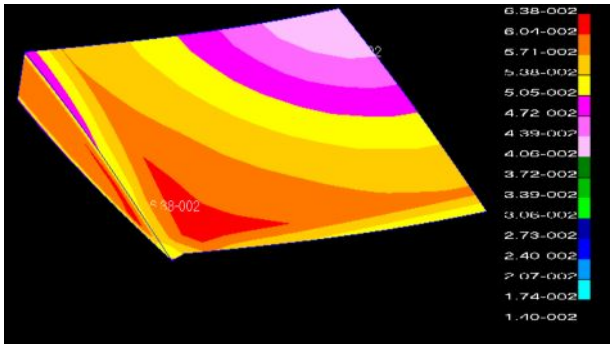

Fig. 4: Distribution of thermal residual stress σ_2 on the 1/16 of X tow

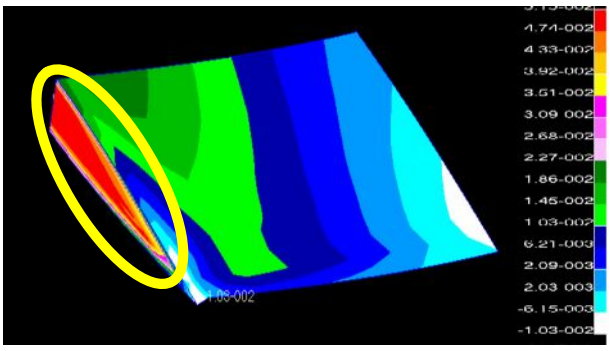

Fig. 5: Distribution of thermal residual stress τ_{31} on the 1/16 of X tow

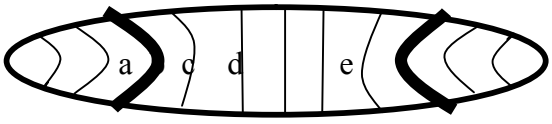

Fig. 6: Cross section of Y fiber tow and predicted location of transverse cracks

5. Composites material's criterion

It is assumed that the transverse cracks occur along both thick lines if all values of the failure criterion in four elements on regions "a" and "b" in Fig. 1 are larger than 1.0. Then the average values of Tsai-Wu's criterion in the regions from "a" to "d", is 1.04, 0.995, 0.959, 0.940, and there isn't a large difference with one another. Since the transverse cracks start from small defects growing in the manufacturing process, it is possible that they might occur everywhere. The values of Hashin's criterion are 1.09, 0.988, 0.916, and 0.877, respectively, and there are large differences among them. From these results, it can be predicted that two transverse cracks have first occurred near the edges and then successive one or two cracks are expected in the center region. This result is more fitted to some experimental results, and it is concluded that Hashin's criterion is more suitable for this study from the comparison.

6. Simulation in the failure process

The results of the simulation in the failure process with Hashin's criterion are as follows. With the applied stress of 31.2 MPa, an element in the Y fiber tow is first judged to be failed and consequently with 75.6 MPa transverse cracks occur in the Y fiber tow along the thick lines shown in Fig. 5 and they are also indicated as yellow lines in Fig. 6 that shows the whole base cell, Here, inside of the red lines, the square region ABCD indicates 1/16 of the base cell where the X fiber tow is stacked over the Y fiber one. With the applied stress of 80.9 MPa, they also start in the X fiber tow as shown as the yellow lines, and consequently progress as shown that the red and green lines mean the states at 97.7 and 119 MPa in Fig. 7. The cracks are predicted to progress from the edges to the center region where the tows become thicker.

Afterwards both the transverse cracks in X and Y fiber tows finally intersect and the delaminations start from their intersections with the applied stress of 158 MPa since the elements in the both tows on that interface are failed. The occurred transverse cracks and delaminations are expressed as the yellow lines and yellow part in Fig. 8. After then, the delaminations extend along the accompanying transverse cracks in both tows as shown that the red, green and orange lines and the parts of each color

mean the states with the applied stresses of 169, 459, and 572 MPa respectively. Then the transverse cracks penetrate the X fiber tow along the width and this causes the large continuous delaminations. Figure 9 illustrates a configuration of the final failure mode with two transverse cracks in each fiber tow and the wide delamination between them. At the same time, the X fiber is predicted to rupture at the point designated with the cross symbol.

The distribution of σ_x and σ_z after the X fiber rupture are given from Fig. 11 to Fig. 14, where they are indicated only in the quarter region of the model shown in Fig. 1 for its symmetry. Figures 11 and Fig. 15 are the the lower left quarter parts and others ore in the upper left parts. The stress concentration of σ_x over 2.0 GPa is observed near the places designated with the cross symbols where the X fiber is predicted to rupture in Fig. 11. On the contrary, as seen in Fig. 13, σ_x is near zero value around the transverse cracks and the stress concentration occurs around the edges of the delaminations. σ_z is zero on the center of the interface of both tows as expressed in Fig. 12 and Fig. 14. The concentration of σ_z is observed in the opposite sides where cannot be seen in these figures. Over all of these figures, the effects in the failures with NSM are calculated with accuracy.

The initiate homogenized elastic properties with no failure are given in table 4. The value of E_y is slightly higher by 10.8% than that of E_x due to lager volume fraction of the Y fiber tow. During the simulation the homogenized elastic properties vary from the successive occurrence of failures as shown as a variation ratio on each property in Fig. 12 and the initial values are given in table 4. The values of E_x and G_{xy} become smaller only 3.36 % and 9.80 % during the simulation, although many transverse cracks that should have an influence on these values penetrated in both fiber tows. Therefore the failures don't affect the in-plain elastic properties fairly. On the other hand, E_z and G_{xz} become smaller by 34.3 % and 17.4 % and they are intensively affected by the onsets of delaminations as shown in Fig. 12. Furthermore it can be considered to become easier to deform in out of plane from observing the increasing values of ν_{xz}.

In addition, the thermal expansion coefficients are also calculated in these axis directions. The values of α_x, α_y and α_z in the initial model are 8.24×10^{-6}, 6.79×10^{-6} and 7.65×10^{-5}. α_x and α_y change into 6.85×10^{-6} and 5.62×10^{-6} in the final failure state, and they are smaller by 16.9 % and 17.2 % respectively. As the failures progress, the thermal residual stresses are released due to the reduction of the mutual constraint. And then the thermal expansion coefficients, α_x and α_y, become smaller than those in the initial state. However, this tendency cannot apply to α_z that changes into 8.26×10^{-5}, grater by 7.93 %. Because of the widely extended delaminations, the model is easier to deform in only out-plane with thermal stresses.

Thus, the behavior of the transverse cracks and the delaminations and the changes in the elastic properties can be clarified throuogh the simulation of the failure process of woven CF/Epoxy laminates.

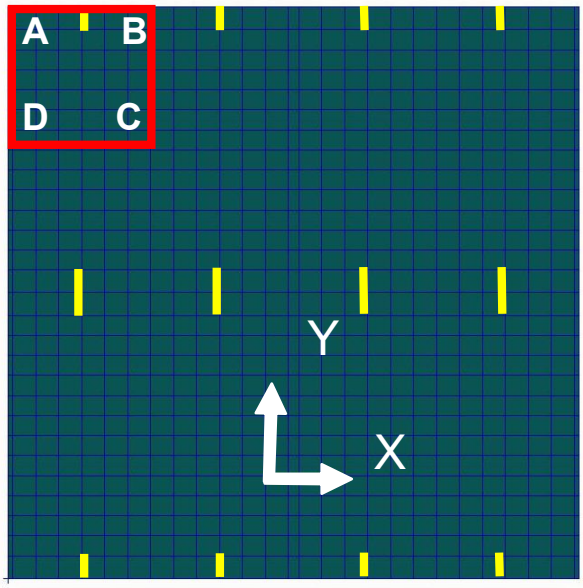

Fig. 7: Base cell
'yellow lines' →occurred transverse cracks in the Y tows, 'red squre ABCD' → the region of 1/4 base cell

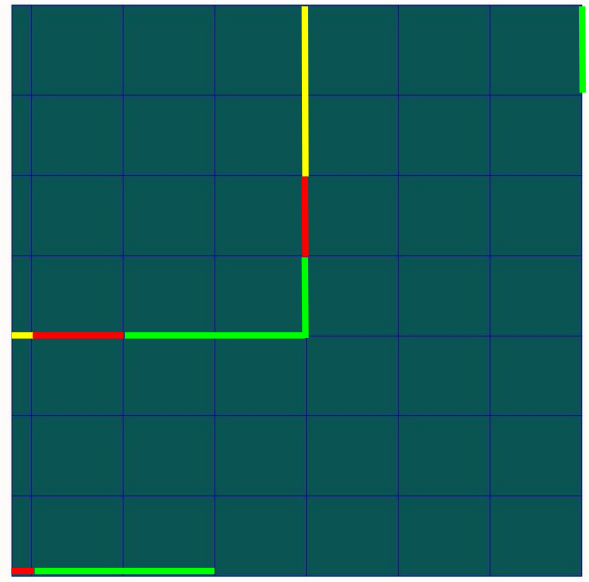

Fig. 8: Occurred transverse cracks, yellow lines →80.9 MPa, red ones →97.7 MPa, green ones → 119 MPa.

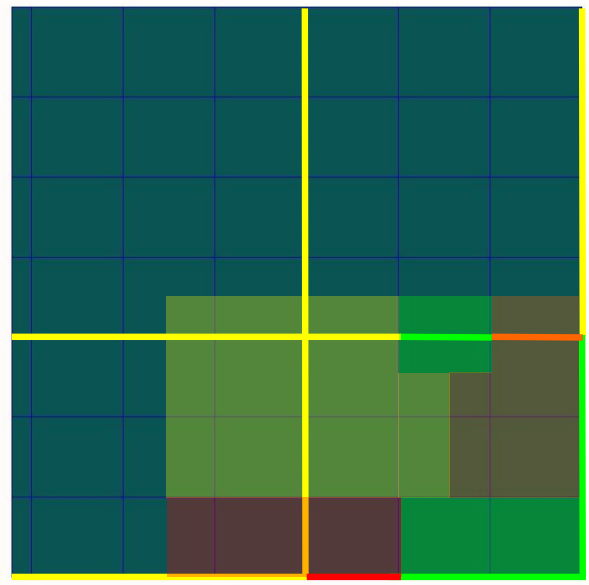

Fig. 9: Places of the occurrences of transverse cracks and delaminaintions
White lines → 119 MPa, Yellow lines and region→ 159 MPa, Red ones → 169 MPa, Green ones → 459 MPa, Orange ones → 472 MPa .

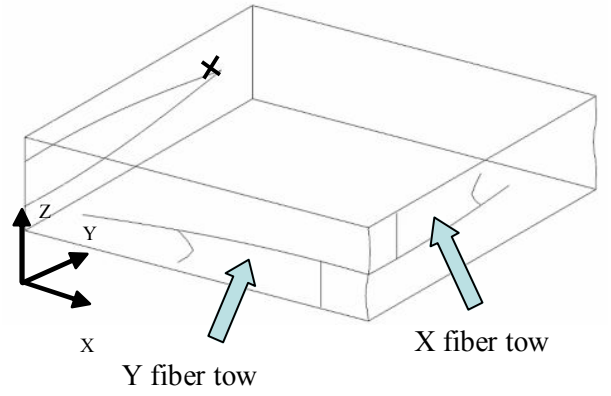

Fig. 10: Final failure mode with the applied stress of 572MPa

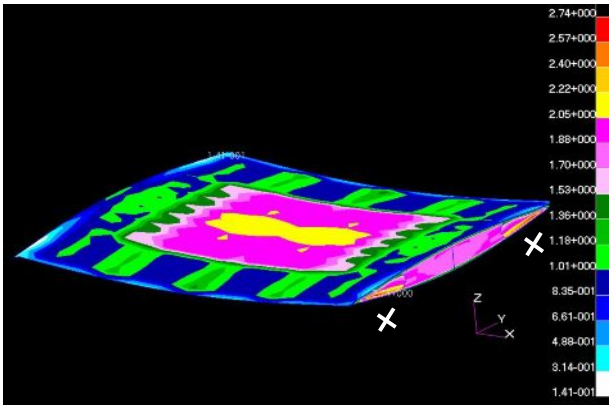

Fig. 11: Distribution of σ_x after the X fibers ruptured on the X fiber tow

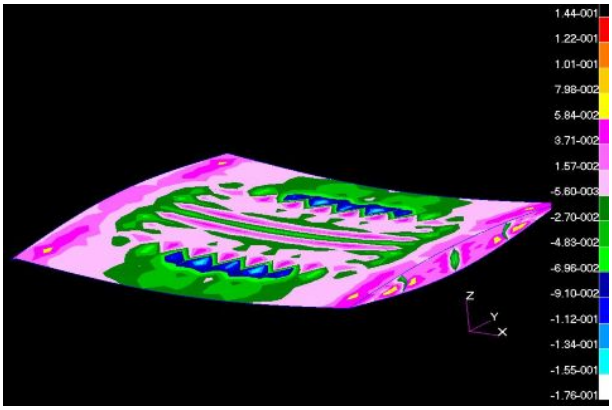

Fig. 12: Distribution of σ_z after the X fiber ruptured on the X fiber tow

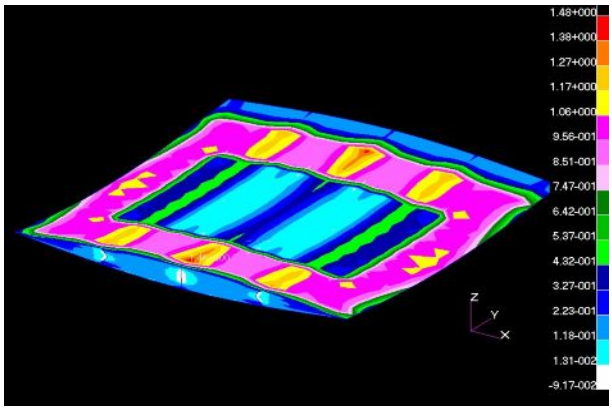

Fig. 13: Distribution of σ_x after the X fiber ruptured on the Y fiber tow

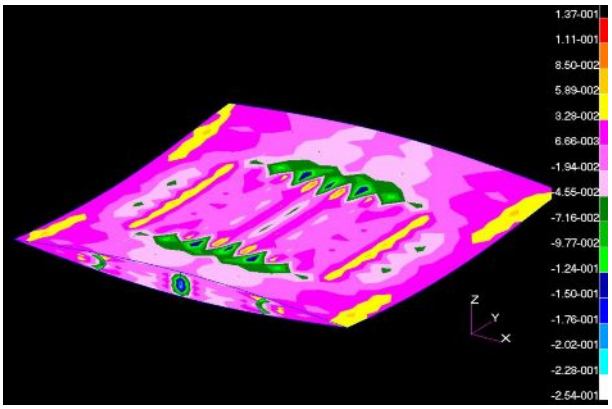

Fig. 14: Distribution of σ_z after the X fiber ruptured on the Y fiber tow

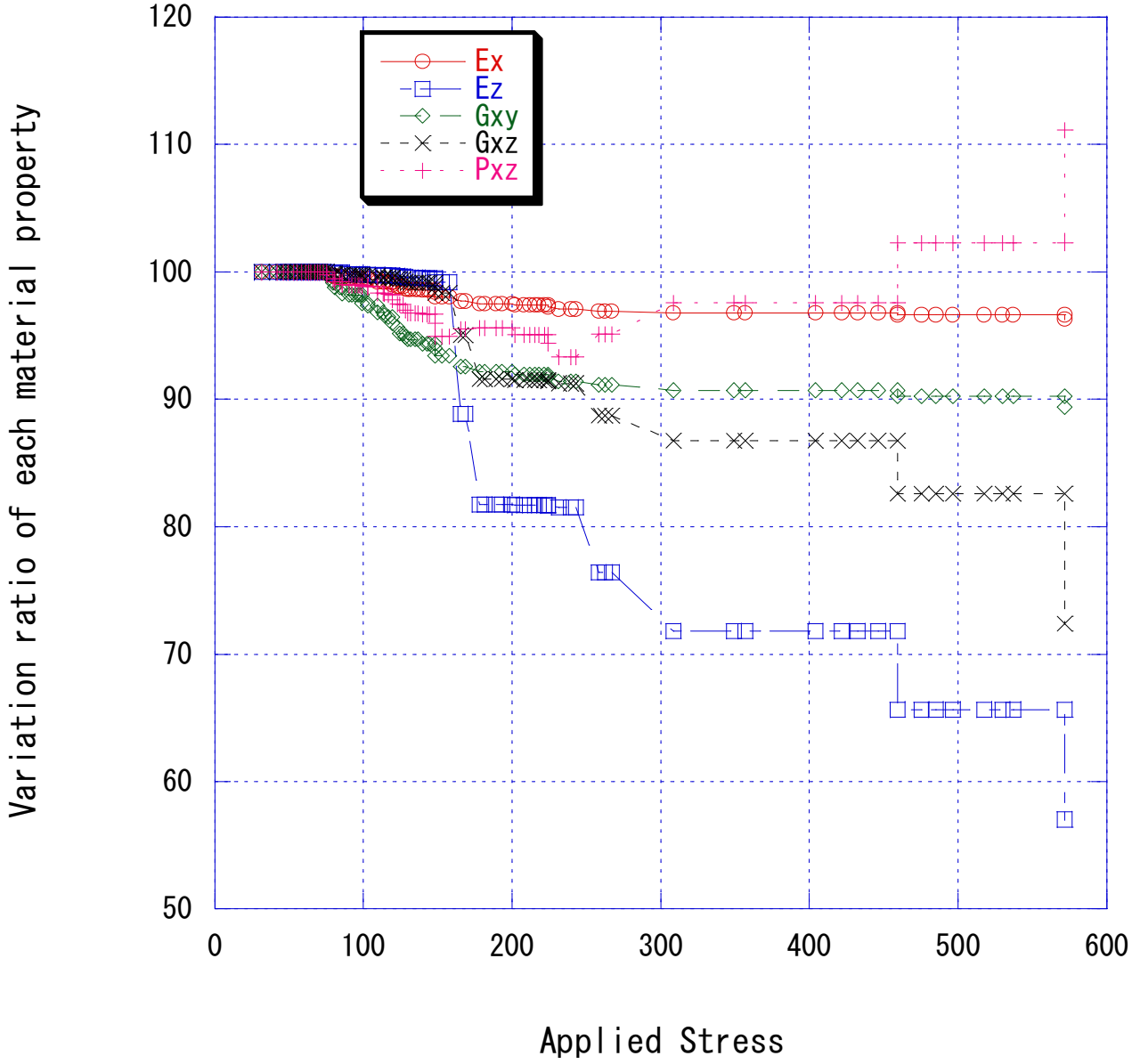

Fig.15: Variation ratio of each material property over the simulation

Table 4 : Homogenaised Elastic properties of Base cell

E_x (GPa)	E_y (GPa)	E_z (GPa)	G_{yz} (GPa)	G_{zx} (GPa)	G_{xy} (GPa)	ν_{yz}	ν_{xz}	ν_{xy}
44.7	50.1	9.79	2.60	2.61	4.77	0.43	0.44	0.14

7. Conclusions

FEM simulation of failure process of CF/Epoxy woven laminates under x-axis tensile force considering the thermal residual stresses calculated by using the homogenization method was carried out to evaluate how important they are and which criteria is the best for this study. To simulate the propagation of transverse cracks in fiber tows and delaminations between them, node separation method was adopted. Under the simulation, the detailed behaviours of the failures were clarified and the stress distributions, the changes in the elastic properties were also investigated. The obtained conclusions are as follows:

1). By comparing simulations with and without thermal residual stresses, it is evident that the thermal residual stresses cannot be neglected in the failure process of woven CF/Epoxy laminates. The maximum tensile stress transverse to the fiber direction σ_2 and maximum shearing stress τ_{31} are observed in the X fiber tow and their values are 63.2MPa amounting to 70.2% of F_{Tt} and 50.5MPa to 56% of S_{Lt}, respectively.

2). Hashin's criterion is more suitable than Tsai-Wu's for this study from the comparison of the predicted location of transverse cracks. Based Hashin's, two transverse cracks have first occurred near the edges and then successive one or two cracks are expected in the center region. On the contrary, they might occur everywhere based on Tsai-Wu's. Since the first one matches some experimental results of woven CF/Epoxy laminate, it can be conclude that Hashin's criterion is more adequate for the simulation.

3). From the simulation, the behaviors of the transverse cracks and the delaminations can be clarified as follows: Two transverse cracks occur near the edges in each fiber tow, first in the Y one and second in the X one. Next the extra one also at the center part in both fiber tows. Afterwards the transverse cracks in both fiber tows intersect and the delaminations start from their intersections and extend along the accompanying transverse cracks in both tows. At the last, the transverse cracks penetrate both fiber tows along the width and this causes the large continuous delaminations. At the same time, the X fiber is predicted to rupture near the edge in the X fiber tow. In addition, it is indicated that the failures have not affected the homogenized elastic properties relating in in-plane fairly, but those of out-plain intensively under the simulation.

8. References

[1] Ishikawa, T. and Chou, T. W., "Elastic behavior of woven hybrid composite."Journal of Composite Materials, Vol.16, 1982, 2-19.

[2] Ishikawa, T. and Chou, T. W., "One-dimensional micromechanical analysis of woven fabric composite." AIAA Journal, Vol.12, 1983, 1714-21.

[3] Naik, N. K. and Ganesh, V. K., "Prediction of on-axis elastic properties of plain weave fabric composites." Composite Science and Technology, Vol.45, 1992, 135-52.

[4] Naik, N. K. and Ganesh, V. K. "Failure behavior of plain weave fabric laminates under On-axis uniaxial loading:II-analytical predictions," Journal of Composite Materials Vol. 30, 1996, 1779-1822

[5] V. K. Ganesh, & Naik, N. K. " Thermal expansion coefficients of plain-weave fabric laminates," Composite Science and Technology, Vol.51, 1994, 387-408

[6] Chapman, C. and Whitcomb, J., "Effect of assumed tow architecture on predicted moduli and stresses in plain weave composite." Journal of Composite Materials, Vol.29, 1995, 2134-59.

[7] Watanabe, N. Oshiba, S and Ishikawa, T. "In-plane mechanical properties of CF/Epoxy 3-D orthogonal interlocked fabric composite" ICCM-12, Paris, France, 1999 CD-ROM.

[8] Kengo Tanaka, Naoyuki Watanabe, "Elasticity and Failure Process of Woven CF/Epoxy Laminates," Proceedings of The Japan Society for Composite Materials, pp.33-34, 2004 (in Japanese).

[9] N. Watanabe and K. Teranishi, "Thermal Stress Analysis for AI Honeycomb Sandwich Plates with Very Thin CFRP Faces", 36th AIAA, Structures, Structures, Structural Dynamics and Materials Conference,

[10] S. W. Tsai & E. M. Wu, "A General Theory of Strength for Anisotropic Materials," Journal of Composite Materials, Vol.5, 1971, pp.58-80

[11] Z. Hashin, "Failure Criteria for Unidirectional Fiber Composites," Journal of Applied Mechanics, Vol.47, 1980, pp.329-33